BMC Chemistry

RESEARCH ARTICLE

Eco-friendly approach to access of quinoxaline derivatives using nanostructured pyrophosphate Na$_2$PdP$_2$O$_7$ as a new, efficient and reusable heterogeneous catalyst

Karim Dânoun[1,2], Younes Essamlali[1], Othmane Amadine[1], Hassan Mahi[1] and Mohamed Zahouily[1,2*]

Abstract

In the present study, we report the synthesis of various quinoxaline derivatives from direct condensation of substituted aromatic 1,2-diamine with 1,2-dicarbonyl catalyzed by nanostructured pyrophosphate Na$_2$PdP$_2$O$_7$ as a new highly efficient bifunctionalheterogeneous catalyst. The quinoxaline synthesis was performed in ethanol as a green and suitable solvent at ambient temperature to afford the desired quinoxalines with good to excellent yields in shorter reaction times. Many Quinoxaline derivatives were successfully synthesized using various 1,2-diketones and 1,2-diamines at room temperature. Catalyst reusability showed that the Na$_2$PdP$_2$O$_7$ catalyst exhibited excellent recyclability without significant loss in its catalytic activity after five consecutive cycles.

Keywords: Nanostructured pyrophosphate, Heterogeneous catalysis, Recyclable catalyst, Quinoxalines, 1,2-Diamine, 1,2-Dicarbonyl

Introduction

Quinoxaline and its derivatives are an important class of heterocyclic compounds, they have attracted considerable attention over the years owing to their very interesting pharmaceutical and biological properties such as insecticidal, antifungal, anthelmintic, anticancer, antibacterial and antiviral [1–6]. Beside their medicinal applications, these compounds have been widely used as dyes, electroluminescent materials, photo-initiators and also in organic semiconductors [7–10]. Recently, much more attention has been devoted to the development of sustainable and efficient methods for the synthesis of quinoxalines derivatives. Over the years, several synthetic strategies have been reported in literature for

the preparation of substituted quinoxalines compounds, some example include the oxidative coupling of epoxides and ene-1,2-diamines [11], the reductive cyclization of 1,2-dicarbonyl compounds with 2-nitroanilines [12], the oxidative cyclization of α-hydroxyketones with *o*-phenylenediamines [13], the coupling of α-diazoketones with aryl 1,2-diamines [14], the reaction of α-haloketones with aromatic 1,2-diamines [15], the intramolecular cyclization of dialdimines [16], and the reaction of aryl-1,2-diamines and diethyl bromomalonate [17]. Furthermore, quinoxaline and its derivatives can also be successfully synthesized from the direct condensation of aryl 1,2-diamines with 1,2-dicarbonyl compounds. Currently, the synthesis of quinoxaline derivatives is usually carried out in the presence of a variety of catalysts. The most commonly used catalysts are polyaniline sulfate salt [18], oxalic acid [19], cerium(IV) ammonium nitrate [20], sulfamic acid [21], Wells–Dawson heteropolyacid [22], bismuth(III) triflate [23], indium chloride [24], ionic

*Correspondence: m.zahouily@mascir.com
[1] Moroccan Foundation for Advanced Science, Innovation and Research (MAScIR), VARENA Center, Rue Mohamed El Jazouli, Madinat Al Irfane, 10100 Rabat, Morocco
Full list of author information is available at the end of the article

liquid 1-*n*-butylimidazolium tetrafluoroborate [25], zirconium tetrabis(dodecylsulfate) [26], palladium(II)acetate [27], gallium(III) triflate [28] and molecular iodine [29]. However, these catalytic systems suffer from several drawbacks, mainly, the drastic reaction conditions such as, high reaction temperature, high catalyst amount, prolonged reaction time even under microwave or ultrasound irradiation, contamination of the product even after purification, and it is impossible to regain the costly catalyst for reuse [30, 31], as well as the environmental pollution caused by the use of a considerable amount of toxic solvents, thus making the process more complicated, expensive, and environmentally unfriendly. Hence, the development of sustainable protocols to design new reusable and efficient heterogeneous catalytic systems that could be used in cleaner process has attracted tremendous interest, and numerous heterogeneous catalytic systems have been reported to be successful for the synthesis of quinoxaline derivatives. ZnO-KIT-6 [32], Ni-nanoparticles [33], Yb/NaY zeolite [34], Al_2O_3 [35], graphene oxide [36], nanocrystalline CuO [37], Nano-TiO_2 [38], montmorillonite K-10 [18]. Another type of materials based on metal phosphates and pyrophosphates are also good candidates for the catalysis of numerous reactions requiring acidic catalysts. These metal pyrophosphates (MP_2O_7) are of a very high interest thanks to their wide range of utilization ranging from ceramics [39] to optical materials [40] and packing materials for chromatographic columns [41]. Among these materials, palladium pyrophosphate has only rarely been explored, for the best of our knowledge, there has not been any report in the literature for the use of a palladium pyrophosphate as a nanocatalyst for the condensation reaction of 1,2-diamine with 1,2-dicarbonyl. Therefore, in continuation of our studies on the development of new efficient synthetic strategies [42, 43], the main objective of the present study is to develop a green and simple route for the synthesis of quinoxaline derivatives from direct condensation between 1,2-diamines and 1,2-dicarbronyl compounds in green solvent at room temperature eover the nano structured $Na_2PdP_2O_7$ as a novel heterogeneous catalyst. Furthermore, the structural, textural, surface and morphological properties of the prepared nanocatalysts, reaction conditions and the nanocatalyst reusability were carefully studied.

Experimental

Materials

All the chemicals are purchased commercially and used without any further purification. The Palladium chloride ($PdCl_2$), sodium phosphate monobasic dehydrate ($NaH_2PO_4 \cdot 2H_2O$), Absolute alcohol, Dichloromethane, Acetonitrile and Ethyl acetate were purchased from Aldrich chemicalcompany.

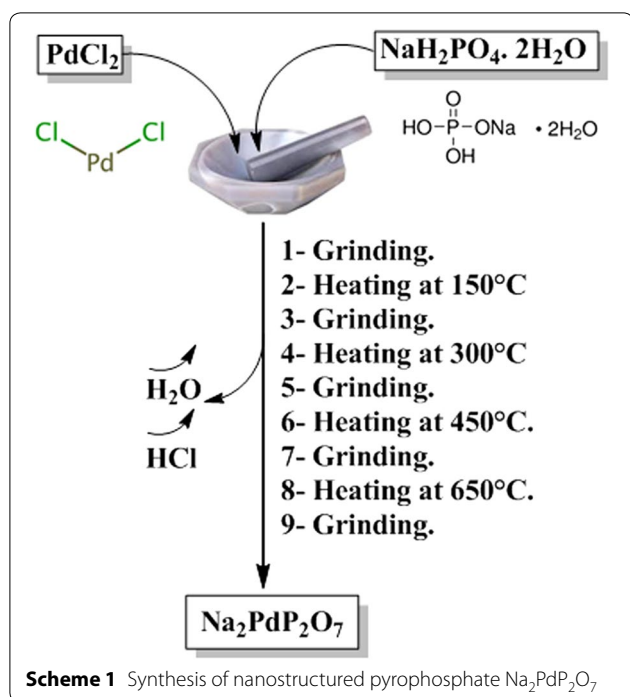### Structural characterization

FTIR spectra of the catalyst were recorded using an ABB Bomem FTLA 2000 spectrometer equipped with a Golden Gate single reflection ATR accessory. Thermal behavior of sample was studied by Thermogravimetric Analysis (TGA) using a Q500 instrument (TA Instruments) with heating rate 10 °C/min, under air atmosphere. X-ray diffraction (XRD) patterns were acquired on a Bruker AXS D-8 diffractometer using Cu K_α source ($\lambda = 1.5418$ Å), operating in Bragg–Brentano geometry (θ–2θ). The SEM micrographs were obtained using FEI Quanta 200 microscope equipped with EDX detector. Transmission electron micrographs were obtained using a FEI microscope operating at accelerating voltage of 120 kV. The specific surface areas were determined from the nitrogen adsorption/desorption isotherm (at −196 °C) using the BET (Brunauer–Emmett–Teller) method. The N_2 adsorption–desorption isotherm data was collected using a Micromeritics 3Flex surface characterization analyzer. Pore size distribution was determined from the N_2 adsorption isotherm according to the Barret, Joyney and Halenda (BJH) theory. NMR spectra were recorded at 14 T on a BrukerAvance III 600 MHz NMR spectrometer, with working frequencies of 600.13 and 150.902 MHz for proton and carbon respectively, using $CDCl_3$as solvent and TMS as the internal standard. The local chemical structure around phosphorus atoms was analyzed by solid-state ^{31}P-nuclear magnetic resonance using magic angle spinning conditions (MAS-NMR) spectroscopy.

Synthesis of the $Na_2PdP_2O_7$ catalyst

The nanostructured pyrophosphate $Na_2PdP_2O_7$ catalyst was prepared by the method recently described in the literature [44], using $NaH_2PO_4 \cdot 2H_2O$ and $PdCl_2$ as starting materials in a molar ratio of 2:1, respectively. Typically, $NaH_2PO_4 \cdot 2H_2O$ and $PdCl_2$ were thoroughly mixed by grindingin an agate mortar to insure better contact opportunity between the components. After grinding, the solid powders were progressively heated in an alumina crucible from room temperature to 650 °C at a heating rate of 10 °C/min, and then rapidly quenched according to the procedure described in Scheme 1. Once the thermal treatment was finished, the obtained yellow powder was ground into fine powder.

General procedure for the preparation of quinoxalines (3a–3h)

Under air atmosphere, an oven-dried round-bottomedflask was charged with equimolar amounts of

Scheme 1 Synthesis of nanostructured pyrophosphate $Na_2PdP_2O_7$

1,2-diamine (1 mmol) and 1,2-diketone (1 mmol). Afterward, ethanol (3 mL) and catalyst (10 mg, 3.06 mol.%) were added and the reaction mixturewas stirred at room temperature for 30 min. The reaction progress was monitored by thin layer chromatography (TLC) using Hexane/ Ethylacetate (9/1) as eluent. After the completion of the reaction, the catalyst was recovered by simple filtration and then repeatedly washed with dichloromethane. The solvent was evaporated under reduced pressure, and the crude product was purified by simple recrystallization in ethanol to yield the desired product.

Results and discussion

Characterization of the catalyst

The FTIR spectrum of the $Na_2PdP_2O_7$ catalyst is depicted in Fig. 1. As shown in this figure, the bands observed at 1180 and 987 cm^{-1}, were assigned to the anti-symmetric and symmetric vibration modes of PO_3 group, respectively. The strong bonds observed at 763 and 910 cm^{-1} and were attributed to the symmetric and anti-symmetric vibrations bands of P–O–P group. Furthermore, the bands appear at around 400–700 cm^{-1} were assigned to the deformation and rocking modes of PO_4 group.

The TGA/DTG analysis of the solid-state mixture of the starting reagents ($NaH_2PO_4 \cdot 2H_2O$ and $PdCl_2$) are presented in Fig. 2. According to TGA curve, the mixture of the starting reagents exhibited four consecutive weight losses. The first weight loss observed below 86 °C can be attributed to the removal of the adsorbed water on the surface of the sample. The second weight loss
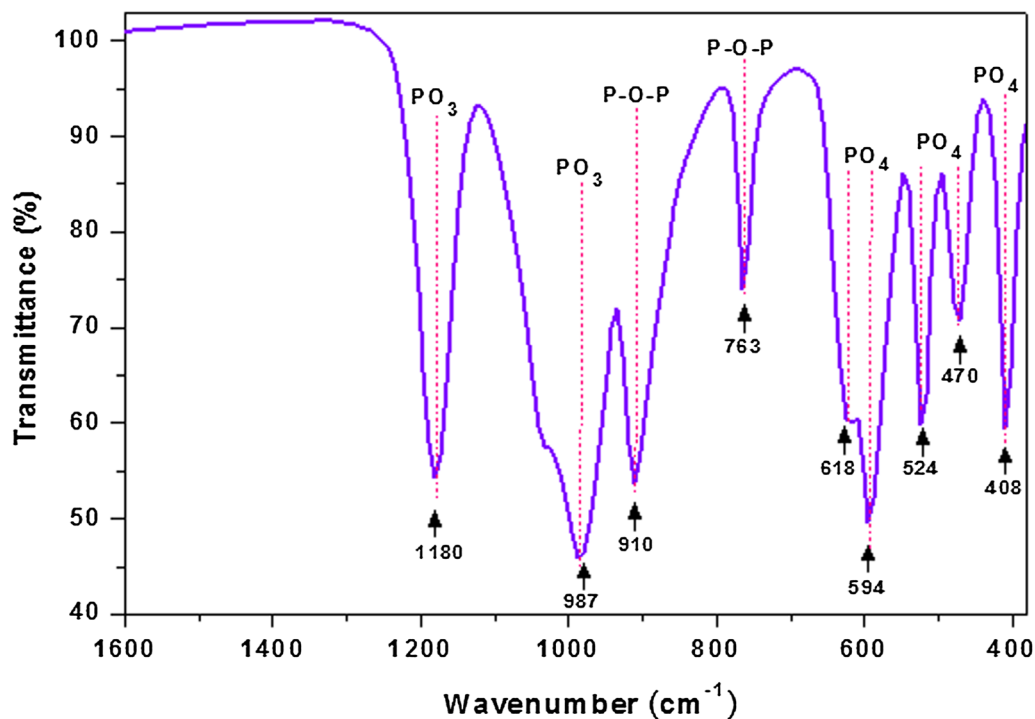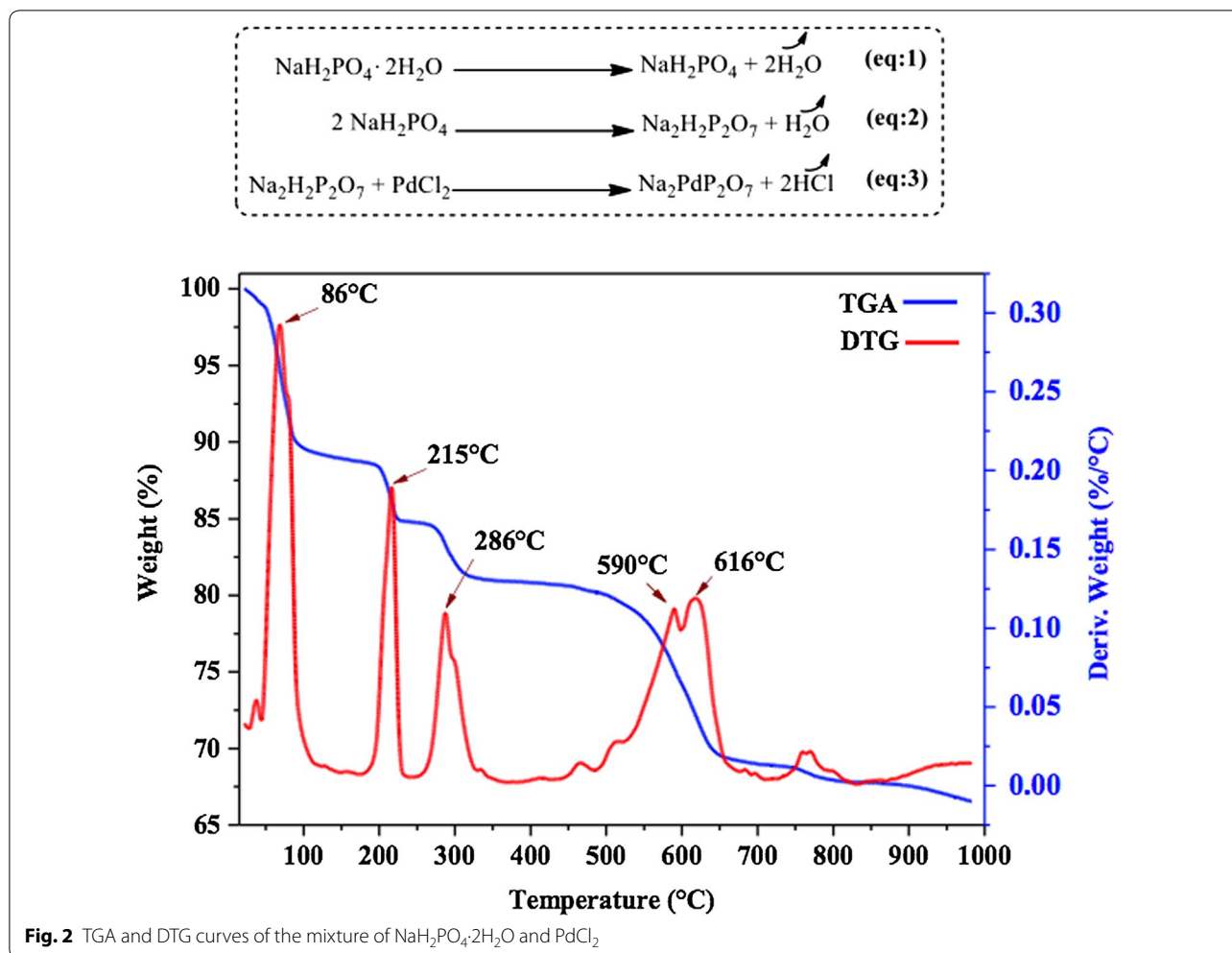

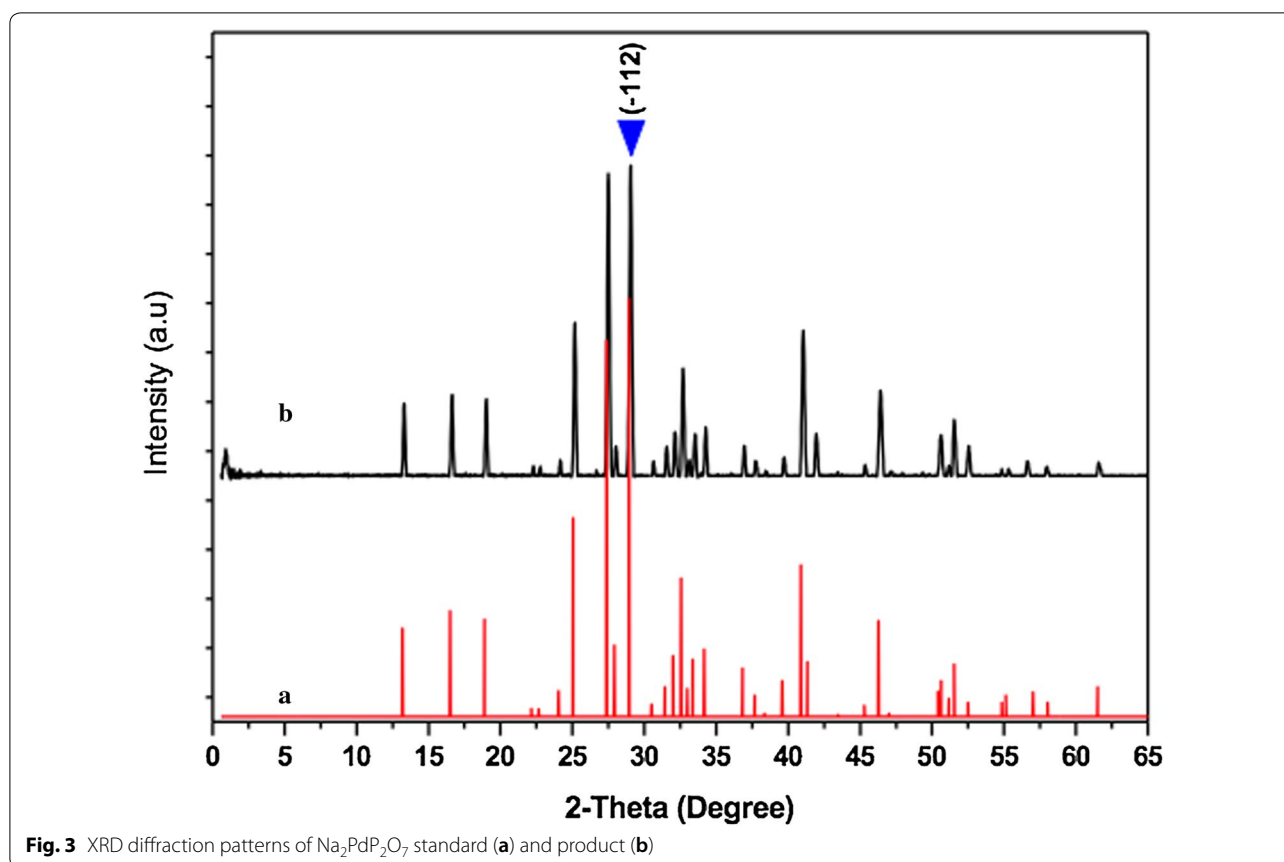
Fig. 1 FT-IR spectrum of nanostructured $Na_2PdP_2O_7$

$$NaH_2PO_4 \cdot 2H_2O \longrightarrow NaH_2PO_4 + 2H_2O \quad \text{(eq:1)}$$

$$2\ NaH_2PO_4 \longrightarrow Na_2H_2P_2O_7 + H_2O \quad \text{(eq:2)}$$

$$Na_2H_2P_2O_7 + PdCl_2 \longrightarrow Na_2PdP_2O_7 + 2HCl \quad \text{(eq:3)}$$

Fig. 2 TGA and DTG curves of the mixture of $NaH_2PO_4 \cdot 2H_2O$ and $PdCl_2$

observed at 215 °C, corresponds to the loss of the two molecules of crystal water in $NaH_2PO_4 \cdot 2H_2O$ (Eq. 1). The third weight loss occurred at the temperature of 286 °C can be assigned to the melting process and the dehydration of NaH_2PO_4 as shown in Eq. 2. It is well known that NaH_2PO_4 dehydrate to acid pyrophosphate at a temperature higher than its melting points [45]. The last weight loss observed at 590 and 616 °C, which may be related to the reaction of melted alkali metal phosphates with palladium chloride according to Eq. 3.

The X-Ray diffraction (XRD) pattern of the as-prepared material is shown in Fig. 3. The XRD pattern of the prepared material indicated that all the diffraction peaks are in good agreement with those of pure $Na_2PdP_2O_7$ according to the JCPDS file No 10-6543 (Fig. 3a). No typical peaks of impurities were observed in the XRD spectrum, indicating single crystal structure of the as-prepared $Na_2PdP_2O_7$ catalyst. Moreover, it was observed that the $Na_2PdP_2O_7$ material exhibited narrow and high peaks

suggesting that the as-prepared $Na_2PdP_2O_7$ is very small in size and has excellent crystallinity. The average crystallite size of the as-prepared $Na_2PdP_2O_7$ material estimated according to the Scherrer equation is about 7.9 nm.

In order to support the aforementioned interpretation [31]PMAS-NMR studies were also investigated. As shown in Fig. 4 , at a rotation frequency of 6 kHz, the isotropic signal was accompanied with other peaks attributed to the rotation bands on the magic angle spinning spectra of the [31]P. These bands became more separated when performing measurement at higher rotation frequency (12 kHz). Furthermore, the presence of one single crystallographic site of phosphorus at a chemical shift of $\delta = 20.11$ ppm, proves the existence of only one type of phosphorus site in the $Na_2PdP_2O_7$ material (Fig. 4b).

The surface morphology of $Na_2PdP_2O_7$ material was studied by scanning electron microscope (SEM) as shown in Fig. 5. The obtained micrographs showed clearly that the surface of $Na_2PdP_2O_7$ is homogeneous in size and

Dânoun *et al. BMC Chemistry*   (2020) 14:6

Page 5 of 13

Fig. 3 XRD diffraction patterns of $Na_2PdP_2O_7$ standard (**a**) and product (**b**)

the shapes and the agglomerates were arranged randomly. Additionally, the surface of these agglomerates is moderately smooth with low visible porosity. This can be explained by a heterogeneous growth of the crystallites caused by the adopted synthesis method, consequently affecting the morphology and porosity.

The as-prepared $Na_2PdP_2O_7$ was analyzed by TEM (Fig. 6). The micrograph obtained showed that the $Na_2PdP_2O_7$ particles were clustered and formed heterogeneous aggregates of nanoparticles that were small in size and irregularly formed (Fig. 6a). By using image J software, the particle size histogram was drawn (from 2.3 to 24 nm), and the mean size of the particles was determined to be around 7 nm (Fig. 6b).
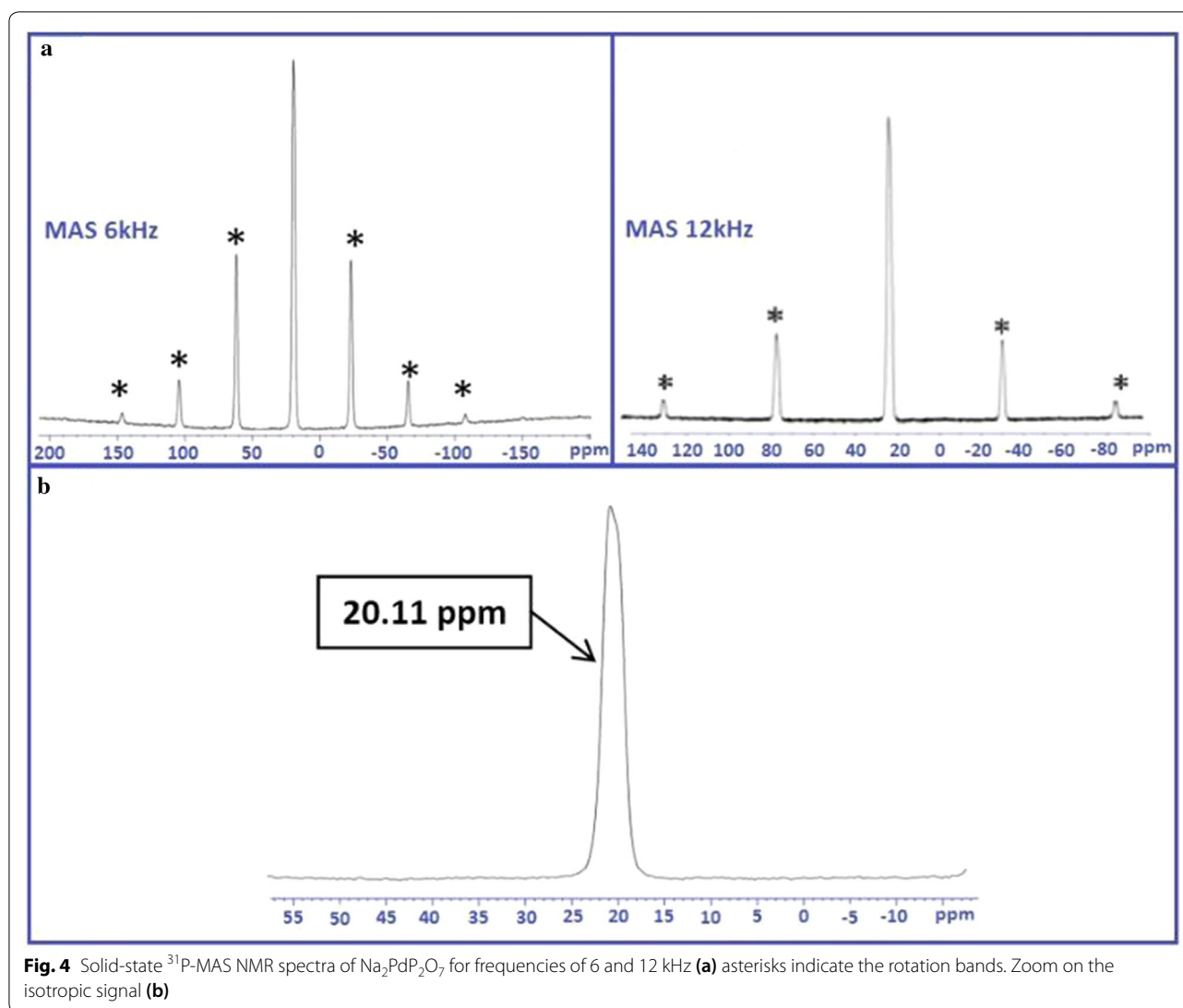
The chemical composition of the as-prepared $Na_2PdP_2O_7$ catalyst was investigated by energy dispersive spectroscopy (EDS). The measurements were performed in two different zones of the sample as shown by the red square in Fig. 7. From EDS analysis, it was confirmed the presence of the characteristic peaks of Na, P, O, and Pd elements in the $Na_2PdP_2O_7$ material. In addition, the results in relative atomic percentages of these elements were found to be closed to those calculated theoretically.

The result in atomic % is as follow: Na: 17.26; Pd: 7.60; P: 17.54; O: 57.60. In addition, no trace of any impurity was detected in EDS spectrum of $Na_2PdP_2O_7$. It is interesting to note that the C and Cu peaks come from the TEM grid.

The surface area of $Na_2PdP_2O_7$ was determined by BET method fromthe nitrogen adsorption–desorption. The BET surface area of the $Na_2PdP_2O_7$ catalyst was found to be 1.16 m^2/g. Indeed, the N_2 adsorption–desorption isotherm shown in Fig. 8a exhibited isotherm type IV according to the IUPAC classification with a distinct hysteresis loop of H2. The BJH pore size distribution (Fig. 10b) revealed that the $Na_2PdP_2O_7$ catalyst exhibits a mesoporous character with the presence of three pore size distribution peaks ranging between 2.52 and 11.84 nm.
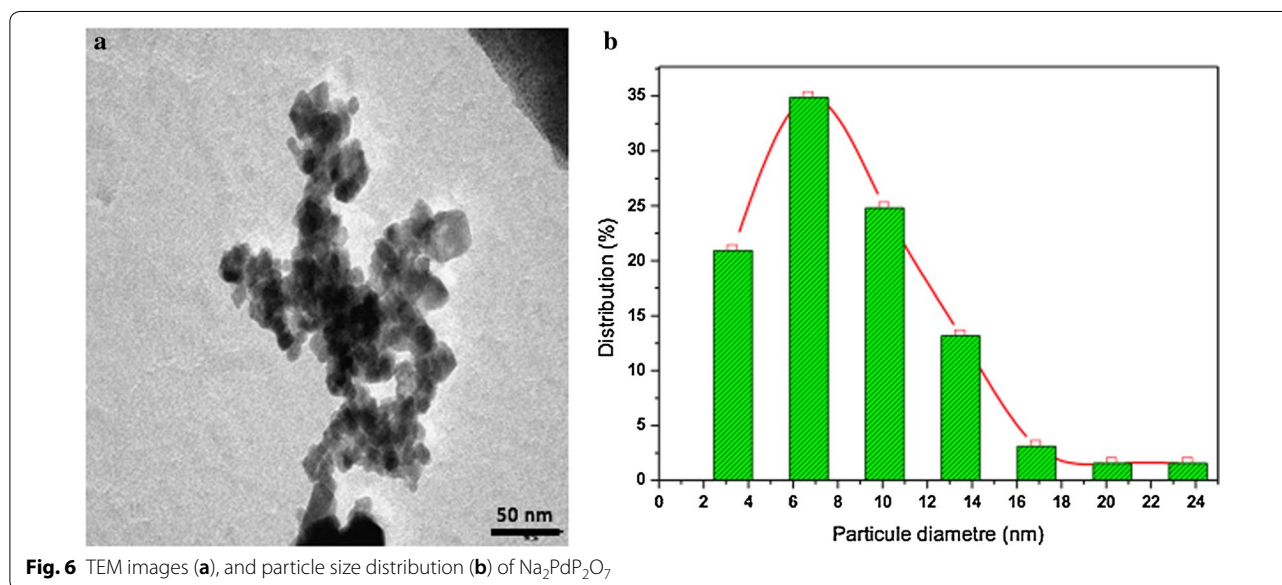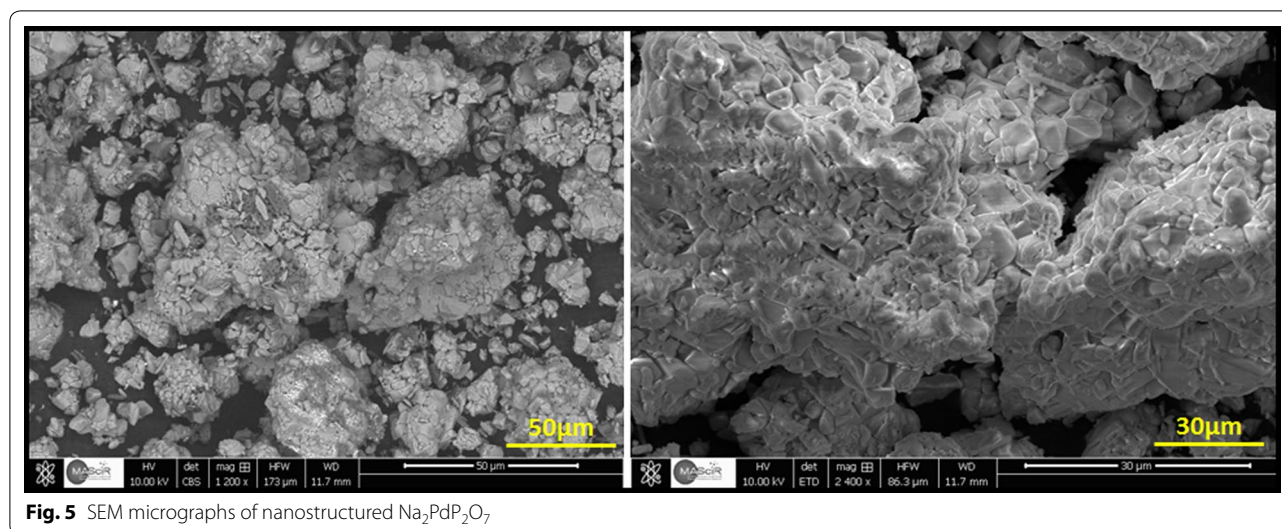
Catalytic activity evaluation

To investigate the catalytic activity of $Na_2PdP_2O_7$ in the condensation reaction, we have studied the model reaction of benzene-1,2-diamine **1a** with benzyl **2a** using ethanol as the solvent in the presence of the nanostructured $Na_2PdP_2O_7$ catalyst (Scheme 2).

Fig. 4 Solid-state ^{31}P-MAS NMR spectra of $Na_2PdP_2O_7$ for frequencies of 6 and 12 kHz **(a)** asterisks indicate the rotation bands. Zoom on the isotropic signal **(b)**

The preliminary experiments were started by screening the activities of some samples. The obtained results of these exploratory experiments are summarized in Fig. 9. Since the

2-diaminobenzene **1a** and benzyl **2a** are very reactive, the condensation reaction between **1a** and **2a** was also carried out without a catalyst under the following reaction condition: 3 mL of ethanol as solvent and at room temperature. As shown in Fig. 9, when the reaction was conducted without a catalyst, the reaction rate was very slow and the yield of **3a** did not exceed 22%. Moreover, the $Na_2CaP_2O_7$ catalyst showed a low catalytic activity, giving only 53% conversion after 30 min. However, using $Na_2PdP_2O_7$ as catalyst gives nearly complete conversion and yielded 98% within 30 min. This result shows the importance of this catalytic system developed in this work.

The effect of various parameters, namely: Temps, nature and volume of the solvent were investigated. Initially we investigated there action of 1,2-diaminobenzene and benzyl over the $Na_2PdP_2O_7$ catalyst in the presence of various solvents namely water, dichloromethane, acetonitrile, ethyl acetate, methanol, propanol and ethanol. The effect of various protic and aprotic solvents on the yield of quinoxaline is depicted in Fig. 10. As shown in this figure, the reaction proceeded comparatively well in aprotic solvent such as dichloromethane (86%), ethyl acetate (87%) and acetonitrile (70%). Among the solvents examined, protic solvents such as alcohols were found to be suitable solvents for quinoxaline synthesis. Excellent yields of the product **3a** were obtained when using 3 mL of propanol (83%) methanol (90%) and ethanol (98%). In the case of water, we obtained moderate yields 49%. This can be explained by the low solubility of the organic
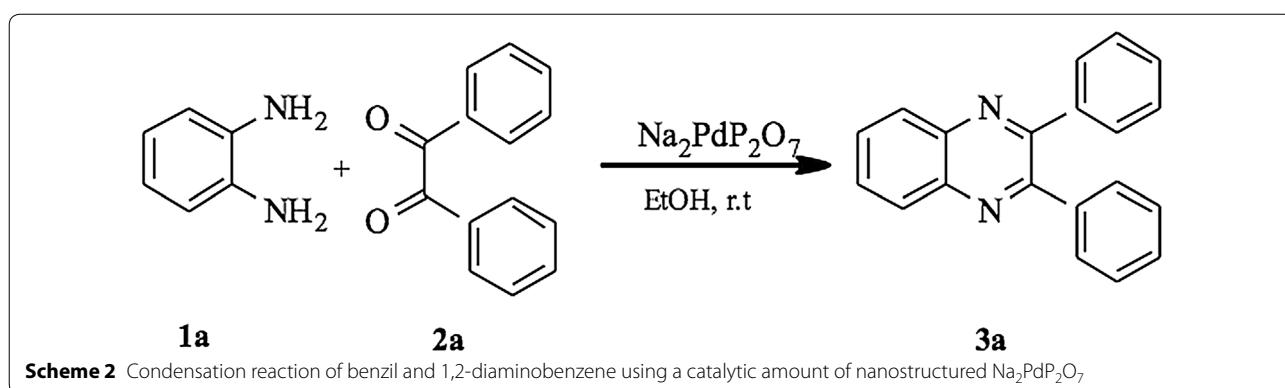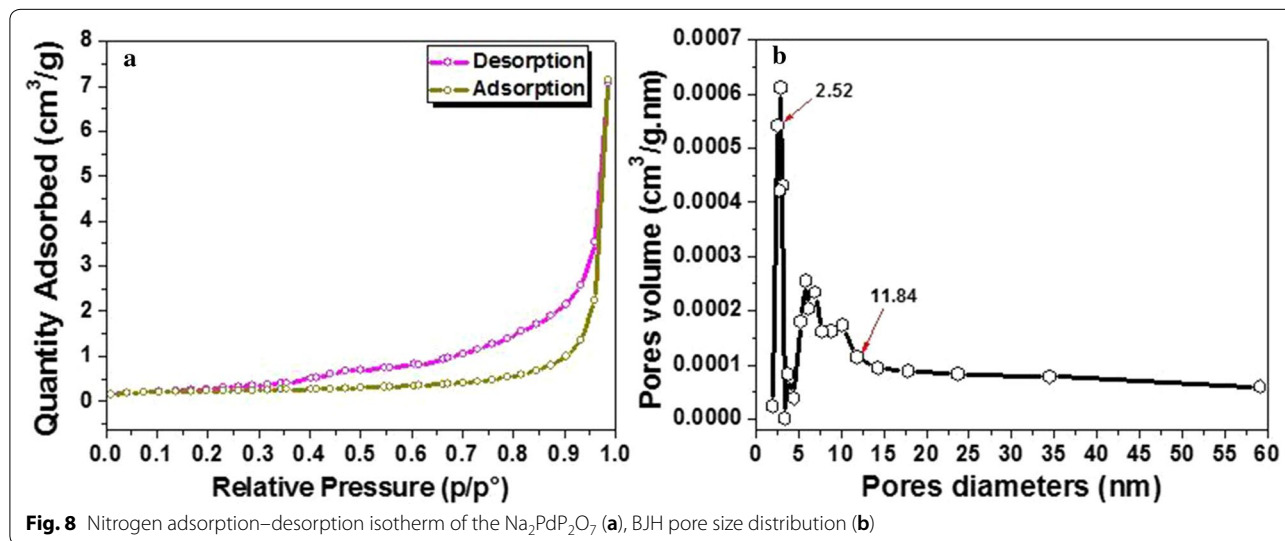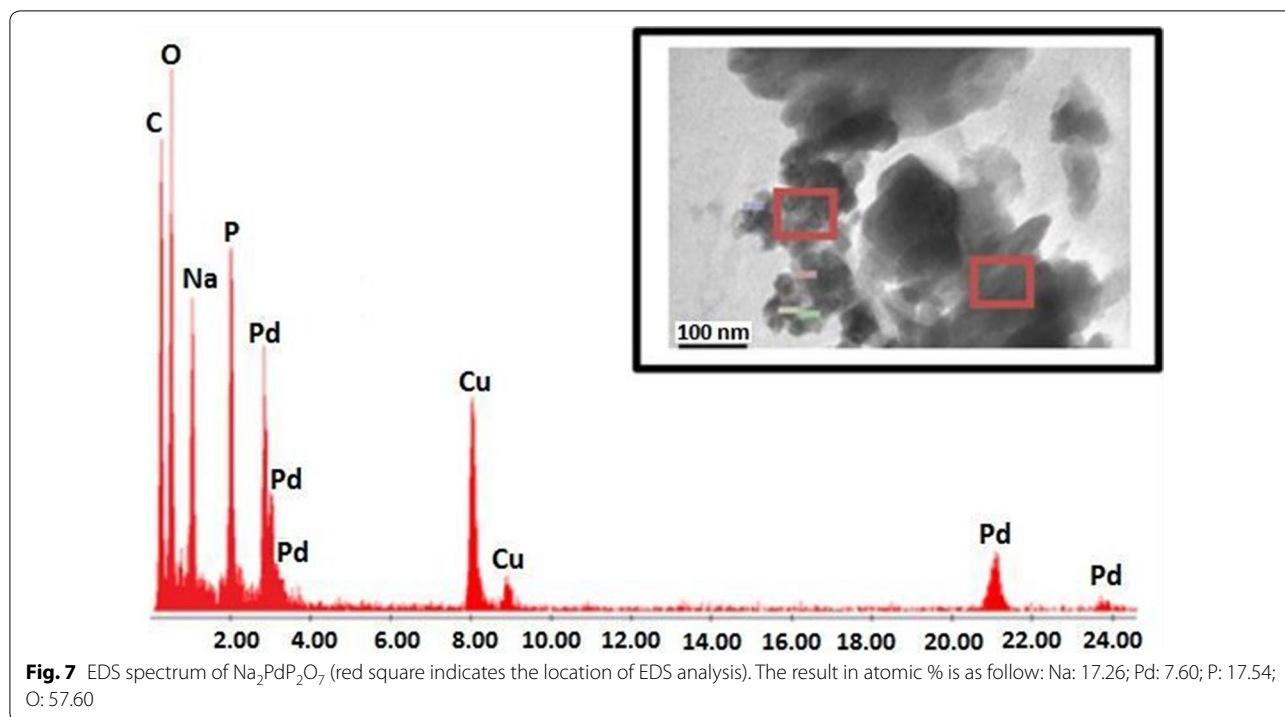
Fig. 5 SEM micrographs of nanostructured $Na_2PdP_2O_7$

Fig. 6 TEM images (**a**), and particle size distribution (**b**) of $Na_2PdP_2O_7$

substrates in water. According to these results, ethanol was considered as the best solvent because of it effective and greener in nature for further studies.

To investigate the effect of the solvent volume on the yield of quinoxaline, the reaction of 1,2-diaminobenzene with benzil was performed at room temperature using 10 mg of catalyst and different volume of ethanol over a period of 30 min, the results are presented in Fig. 11. As can be seen from this Figure, the quinoxaline yield increased drastically with increasing volume of ethanol until an optimum value of 3 mL and then decreased gradually. Indeed, when the volume of ethanol was increased from 1 to 3 mL, the reaction yield increased from 76 to

98%. However, further increase in the volume of the ethanol up to 6 mL resulted in a significant drop in the quinoxaline yield (72% yield for 6 mL). This drop-in product yield can probably be due to the dilution phenomenon and to the high dispersion of the reagents when large volume of ethanol was used.

The effect of the reaction time was also investigated from 5 to 40 min (Fig. 12). As shown in this figure, the nanostructured $Na_2PdP_2O_7$ is the best catalyst compared with $Na_2CaP_2O_7$ and in the absence of any catalyst. When the reaction time was 5 min, the yield was modest (62%). The increase in reaction time induced a significant increase in yield. The optimal time for the condensation
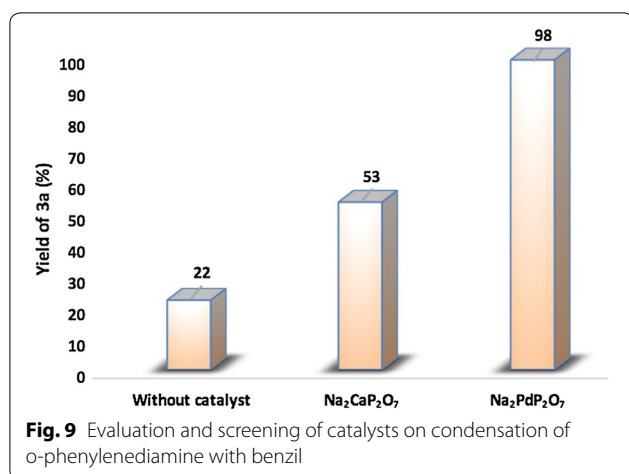
Fig. 7 EDS spectrum of $Na_2PdP_2O_7$ (red square indicates the location of EDS analysis). The result in atomic % is as follow: Na: 17.26; Pd: 7.60; P: 17.54; O: 57.60

Fig. 8 Nitrogen adsorption–desorption isotherm of the $Na_2PdP_2O_7$ (**a**), BJH pore size distribution (**b**)

Scheme 2 Condensation reaction of benzil and 1,2-diaminobenzene using a catalytic amount of nanostructured $Na_2PdP_2O_7$

Dânoun *et al. BMC Chemistry*   (2020) 14:6

Page 9 of 13

Fig. 9 Evaluation and screening of catalysts on condensation of o-phenylenediamine with benzil

Fig. 10 Effect of different solvents on the quinoxaline yield

Reaction conditions:
T°C = room temperature; solvent (3 mL); mole ratio = 1:1 (diamine/benzil);
amount of catalyst = 10 mg, reaction time= 30 min.

Fig. 11 Effect of the volume of ethanol in the synthesis of quinoxaline **3a**

Fig. 12 Kinetic study of the synthesis of quinoxaline **3a** catalyzed by nanostructured $Na_2PdP_2O_7$, $Na_2CaP_2O_7$ and without catalyst, respectively
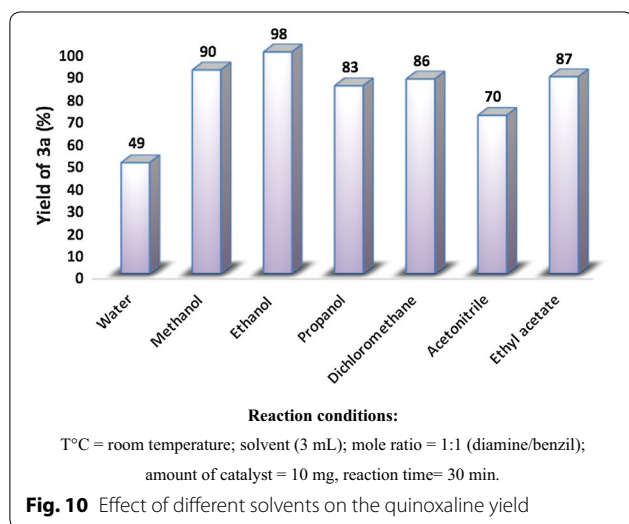
Table 1 Synthesis of quinoxaline derivatives using nanostructured $Na_2PdP_2O_7$

Entry	Amine	1,2-Dicarbonyl	Product	Yield[a] (%)
1			**3a**	98
2			**3b**	95
3			**3c**	81
4			**3d**	86
5			**3e**	91
6			**3f**	86
7			**3g**	77
8			**3h**	80

Reaction condition: diketone (1 mmol), diamine (1 mmol), 10 mg of $Na_2PdP_2O_7$, ethanol (3 mL) and stir rt

[a] Isolated yield

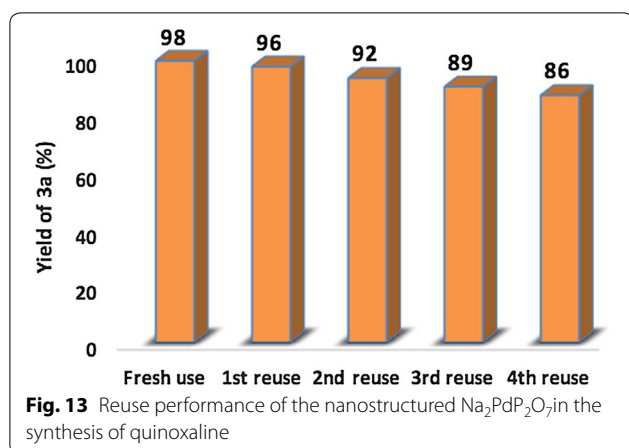**Scheme 3** A proposed mechanism for the synthesis of 2,3-diphenylquinoxaline **3a**

of o-phenylenediamine with benzyl is 30 min, over this period of time, the yield does not evolve anymore.

Encouraged by the remarkable results obtained with the above optimized reaction conditions, we looked at examine the utility of this methodology in order to generalize the reaction with various substituted 1,2-diamine and 1,2-dicarbonyl compounds over the prepared

$Na_2PdP_2O_7$ catalyst; the obtained results are summarized in Table 1. As illustrated in this Table, most of the reactions preceded very effectively at room temperature and no undesirable side-reactions were observed, although the yields were highly dependent on the substrate used. Indeed, the presence of electron-donating substituent such as methyl group on benzene-1,2-diamine substrate

Dânoun *et al. BMC Chemistry*   (2020) 14:6

Page 11 of 13

Fig. 13 Reuse performance of the nanostructured $Na_2PdP_2O_7$ in the synthesis of quinoxaline

did not affect the reaction time and thus no significant difference in quinoxaline derivative yield was observed (Entry 2), while electron withdrawing substituents present in the benzene-1,2-diamines substrate (Entries 3 and 4) decreased the rate of reaction notably, and the corresponding yields were also low as compared to unsubstituted benzene-1,2-diamine. On the other hand, the reaction between aliphatic 1,2-dicarbonyl compounds such as biacetyl (Entries 5–8) with benzene-1,2-diamine containing electron-donating groups such as methyl group provided a good yield (Entry 6), while electron withdrawing substituent gave a satisfactory yield (Entry 7–8). According to the obtained results, we noticed that the aliphatic carbonyls substrates are less reactive than aromatic diketones.

One of the key points to understand the reaction mechanism in heterogeneous catalysis is the determination of the active catalytic sites. The $Na_2PdP_2O_7$ is expected to be a bifunctional catalyst owing to the presence of both acid and basic sites such as $P_2O_7^{4-}$, PO_4^{3-}, Na^+ and Pd^{2+}. We suggest that the condensation reaction occurs over both acid sites and basic sites involved in the $Na_2PdP_2O_7$ catalyst. The plausible mechanism for this reaction was proposed in Scheme 3. The reaction mechanism occurs in three steps: 1,2-diketone was initially activated by the acidic sites of the $Na_2PdP_2O_7$ catalyst (i). Afterward, nucleophilic attack by the amino group involved in the benzene-1,2-diamine on the activated 1,2-diketones generated the 2,3-diphenyl-1,2,3,4-tetrahydro-quinoxaline-2,3-diol as an intermediate (ii); internal rearrangement, followed by elimination of two water molecules, resulted in the formation of the quinoxaline **3a** (iii).

The reusability of the catalyst is one of the most important features of a heterogeneous catalyst especially from an economic and environmental point of view. For this purpose, a recycling study of the $Na_2PdP_2O_7$ catalyst was conducted using the condensation reaction between the benzene-1,2-diamine with benzil as a model reaction. After each cycle, the $Na_2PdP_2O_7$ catalyst was recovered by simple filtration, washed with dichloromethane, dried at 100 °C overnight and then directly reused in the next run under similar reaction condensations. Fifth consecutive runs were performed and the obtained results are shown in Fig. 13. As can be seen, there used catalyst showed a slight decrease in its catalytic activity during the first three runs. However, a significant decrease in the quinoxaline yield was observed after five consecutive runs. This a partial deactivation of the catalyst can be explained by the adsorbed reactants on the surface of the $Na_2PdP_2O_7$ catalyst, which poison the catalytic surface of the catalyst and hinder the reagents to access to the active sites.

Conclusions

In conclusion, the present work propose a simple and green synthetic methodology for the synthesis of quinoxaline and its derivatives by the direct condensation of 1,2-dicarbonyl with substituted aryl 1,2-diamines, using nanostructured $Na_2PdP_2O_7$ as a highly efficient heterogeneous catalyst. Under optimized conditions, our developed nanostructured catalyst showed high catalytic activity using ethanol as a green solvent at room temperature. The easy work-up, short reaction time, good yield of the desired products and eco-friendly process are the noteworthy features of our synthesis procedure. Furthermore, the catalyst can be easily separated from the reaction mixture and directly reused in several cycles with only a slight drop in its catalytic activity. For practical application, the heterogeneous $Na_2PdP_2O_7$ catalyst appeared to be promising candidate to replace the conventional homogeneous and expensive heterogeneous catalysts, currently used in the synthesis of various industrially important and biologically active quinoxalines.

Supplementary information

Additional file 1. Analytical and physicochemical data of quinoxaline derivatives **3a–3h**.

Abbreviations

FTIR: Fourrier Transform infrared; XRD: X-ray diffraction; TGA: Thermogravimetric analyses; SEM: Scanning electron microscope; TEM: Transmission electron microscope; IUPAC: International Union of Pure and Applied Chemistry; EDS: Energy dispersive spectroscopy; ^{1}HNMR: Proton nuclear magnetic resonance spectroscopy; ^{13}CNMR: Carbon nuclear magnetic resonance spectroscopy; $CDCl_3$: Deuterochloroform; TMS: Tetramethylsilane; MAS-NMR: Magic angle spinning in solid-state NMR spectroscopy; KBr: Potassium bromide.

Dânoun *et al. BMC Chemistry*   (2020) 14:6

Page 12 of 13

Author details
^{1} Moroccan Foundation for Advanced Science, Innovation and Research (MAScIR), VARENA Center, Rue Mohamed El Jazouli, Madinat Al Irfane, 10100 Rabat, Morocco. ^{2} University Hassan II Casablanca, FST Mohammedia, Laboratory of Materials, Catalysis and Valorization of Natural Resources - URAC 24, B.P. 146, 20650 Casablanca, Morocco.

References
1. Corona P, Carta A, Loriga M, Vitale G, Paglietti G (2009) Synthesis and in vitro antitumor activity of new quinoxaline derivatives. Eur J Med Chem 44:1579–1591
2. Kotharkar SA, Shinde DB (2006) Synthesis of antimicrobial 2,9,10-trisubstituted-6-oxo-7,12-dihydro-chromeno[3,4-b]quinoxalines. Bioorg Med Chem Lett 16:6181–6184
3. Ganapathy S, Ramalingam P, Baburao C (2008) Antimicrobial and anti-mycobacterial activity of some quinoxalines 'N' bridgehead heterocycles. Asian J Chem 20:3353–3356
4. Khan SA, Saleem K, Khan Z (2007) Synthesis, characterization and in vitro antibacterial activity of new steroidal thiazoloquinoxalines. Eur J Med Chem 42:103–108
5. Guillon J, Forfar IM, Matsuda M, Desplat V, Saliège M, Thiolat D, Massip S, Tabourier A, Léger JM, Dufaure B, Haumont G, Jarry C, Mossalayi D (2007) Synthesis, analytical behaviour and biological evaluation of new 4-substituted pyrrolo[1,2-a]quinoxalines as antileishmanial agents. Bioorg Med Chem. 15:194–210
6. Kakanejadifard A, Zabardasti A, Ghasemian M, Toosi-Jamali H (2008) Synthesis and characterization of Cd(II), Zn(II) and Hg(II) chloride adducts of (2Z,3Z)-1,4,7- trithiononane-2,3-dionedioxime. Asian J Chem 20:1473–1476
7. Brock ED, Lewis DM, Yousaf TI, Harper HH. The Procter and Gamble Company, USA WO 9951688, 1999
8. Thomas KRJ, Velusamy M, Lin JT, Chuen CH, Tao YT (2005) Chromophore-labeled quinoxaline derivatives as efficient electroluminescent materials. Chem Mater 17:1860–1866
9. Balta DK, Keskin S, Karasu F, Arsu N (2007) Quinoxaline derivatives as photoinitiators in UV-cured coatings. Prog Org Coat 60:207–210
10. Dailey S, Feast WJ, Peace RJ, Sage IC, Till S, Wood EL (2001) Synthesis and device characterisation of side-chain polymer electron transport materials for organic semiconductor applications. J Mater Chem 11:2238–2243
11. Antoniotti S, Duñach E (2002) Direct and catalytic synthesis of quinoxaline derivatives from epoxides and ene-1,2-diamines. Tetrahedron Lett 43:3971–3973
12. Shi DQ, Dou GL, Ni SN, Shi JW, Li XY (2008) An efficient synthesis of quinoxaline derivatives mediated by stannous chloride. J Heterocycl Chem 45:1797–1801
13. Robinson RS, Taylor RJK (2005) Quinoxaline synthesis from α-hydroxy ketones via a tandem oxidation process using catalysed aerobic oxidation. Synlett 6:1003–1005
14. Yadav JS, Reddy BVS, Rao YG, Narsaiah AV (2008) First example of Cu(OTf)$_2$-catalyzed synthesis of quinoxalines from α-diazoketones and aryl 1,2-diamines. Chem Lett 37:348–349
15. Wu HW, Yang GS (2008) One-pot synthesis of quinoxalines from alpha-haloketones and aromatic 1, 2-diamines via an oxidation-condensation process. Chin J Org Chem. 28:2132–2136
16. Reich BJE, Justice AK, Beckstead BT, Reibenspies JH, Miller SA (2004) Cyanide-catalyzed cyclizations via aldimine coupling. J Org Chem 69:1357–1359
17. Haldar P, Dutta B, Guin J, Ray JK (2007) Uncatalyzed condensation between aryl-1,2-diamines and diethyl bromomalonate: a one-pot access to substituted ethyl 3-hydroxyquinoxaline-2-carboxylates. Tetrahedron Lett 48:5855–5857
18. Huang TK, Wang R, Shi L, Lu XX (2008) Montmorillonite K-10: an efficient and reusable catalyst for the synthesis of quinoxaline derivatives in water. Catal Commun 9:1143–1147
19. Srinivas C, Kumar CNSSP, Rao VJ, Palaniappan S (2007) Efficient, convenient and reusable polyaniline-sulfate salt catalyst for the synthesis of quinoxaline derivatives. J Mol Catal Chem 265:227–230
20. Hasaninejad A, Zare A, Mohammadizadeh MR, Shekouhy M (2008) Oxalic acid as an efficient, cheap, and reusable catalyst for the preparation of quinoxalines via condensation of 1,2-diamines with α-diketones at room temperature. Arkivoc xiii:28–35
21. More SV, Sastry MNV, Yao CF (2006) Cerium (IV) ammonium nitrate (CAN) as a catalyst in tap water: a simple, proficient and green approach for the synthesis of quinoxalines. Green Chem 8:91–95
22. Li Z, Li W, Sun Y, Huang H, Ouyang P (2008) Room temperature facile synthesis of quinoxalines catalyzed by amidosulfonic acid. J Heterocycl Chem 45:285–288
23. Heravi MM, Bakhtiari K, Bamoharram FF, Tehrani MH (2007) Wells-Dawson type heteropolyacid catalyzed synthesis of quinoxaline derivatives at room temperature. Monatsh Chem 138:465–467
24. Yadav JS, Reddy BVS, Premalatha K, Shankar KS (2008) Bismuth(III)-catalyzed rapid synthesis of 2,3-disubstituted quinoxalines in water. Synthesis 23:3787–3792
25. Hazarika P, Gogoi P, Konwar D (2007) Efficient and green method for the synthesis of 1,5-benzodiazepine and quinoxaline derivatives in water. Synth Commun 37:3447–3454
26. Potewar TM, Ingale SA, Srinivasan KV (2008) Efficient synthesis of quinoxalines in the ionic liquid 1-*n*-butylimidazolium tetrafluoroborate ([Hbim]BF$_4$) at ambient temperature. Synth Commun 38:3601–3612
27. Hasaninejad A, Zare A, Zolfigol MA, Shekouhy M (2009) Zirconium Tetrakis (dodecyl Sulfate) [Zr(DS)4] as an efficient lewis acid-surfactant combined catalyst for the synthesis of quinoxaline derivatives in aqueous media. Synth Commun 39:569–579
28. Cai JJ, Zou JP, Pan XQ, Zhang W (2008) Gallium(III) triflate-catalyzed synthesis of quinoxaline derivatives. Tetrahedron Lett 49:7386–7390
29. Bhosale RS, Sarda SR, Ardhapure SS, Jadhav WN, Bhusare SR, Pawar RP (2005) An efficient protocol for the synthesis of quinoxaline derivatives at room temperature using molecular iodine as the catalyst. Tetrahedron Lett 46:7183–7186
30. Guo WX, Jin HL, Chen JX, Chen F, Ding JC, Wu HY (2009) An efficient catalyst-free protocol for the synthesis of quinoxaline derivatives under ultrasound irradiation. J Braz Chem Soc 20:1674–1679
31. Zhao Z, Wisnoski DD, Wolkenberg SE, Leister WH, Wang Y, Lindsley CW (2004) General microwave-assisted protocols for the expedient synthesis of quinoxalines and heterocyclic pyrazines. Tetrahedron Lett 45:4873–4876
32. Oveisi H, Adharvana MC, Chi VN, Jeffrey EC, Saad MA, Ekrem Y, Shahriar AHM, Yusuke Y, Kevin CWW (2017) ZnO-loaded mesoporous silica (KIT-6) as an efficient solid catalyst for production of various substituted quinoxalines. Catal Commun 90:111–115

Dânoun *et al. BMC Chemistry*   (2020) 14:6

Page 13 of 13

33. Ajeet K, Santosh K, Amit S, Arnab D, Subho M (2008) Ni-nanoparticles: an efficient catalyst for the synthesis of quinoxalines. Catal Commun 9:778–784

34. Fan LY, Wei L, Hua WJ, Li XX (2014) Yb modified NaY zeolite: a recyclable and efficient catalyst for quinoxaline synthesis. Chin Chem Lett 25:1203–1206

35. Jafarpour M, Rezaeifard A, Danehchin M (2011) Easy access to quinoxaline derivatives using alumina as an effective and reusable catalyst under solvent-free conditions. Appl Catal A Gen 394:48–51

36. Roy B, Ghosh S, Ghosh P, Basu (2015) Graphene oxide (GO) or reduced graphene oxide (rGO): efficient catalysts for one-pot metal-free synthesis of quinoxalines from 2-nitroaniline. Tetrahedron Lett 56:6762–6767

37. Sadjadi S, Sadjadi S, Hekmatshoar R (2010) Ultrasound-promoted greener synthesis of benzoheterocycle derivatives catalyzed by nanocrystalline copper(II) oxide. Ultrason Sonochem 17:764–767

38. Mirjalili BBF, Akbari A (2011) Nano-TiO_2: an eco-friendly alternative for the synthesis of quinoxalines. Chin Chem Lett 22:753–756

39. Sato Y, Shen Y, Nishida M, Kanematsu W, Hibino T (2012) Proton conduction in non-doped and acceptor-doped Metal pyrophosphate (MP_2O_7) composite ceramics at intermediate temperatures. J Mater Chem 22:3973–3981

40. Zhang YC, Cheng W, Wu D, Zhang H, Chen D, Gong Y, Kan Z (2004) Crystal and band structures, bonding, and optical properties of solid compounds of alkaline indium (III) pyrophosphates MInP2O7(M = Na, K, Rb, Cs). Chem Mater 16:4150–4159

41. Inoue S, Nobuyuki O. Stationary phase material for chromatography. US 5728463 A, 1988

42. Dânoun K, Jioui I, Bouhrara M, Zahouily M, Solhy A, Jouiad M, Len C, Fihri A (2015) Nano-structured pyrophosphate $Na_2CaP_2O_7$ as catalyst for selective synthesis of 1,2-disubstituted benzimidazoles in pure water. Curr Org Chem 19:2132–2141

43. Jioui I, Dânoun K, Solhy A, Jouiad M, Zahouily M, Essaid B, Len C, Fihri A (2016) Modified fluorapatite as highly efficient catalyst for the synthesis of chalcones via Claisen-Schmidt condensation reaction. J Ind Eng Chem 39:218–225

44. Dânoun K, Essamlali Y, Amadine O, Tabit R, Fihri A, Len C, Zahouily M (2018) Nanostructured pyrophosphate Na2PdP2O7-catalyzed Suzuki-Miyaura cross-coupling under microwave irradiation. Appl Organomet Chem 32:1

45. Perry DL, Phillips SL (1998) Handbook of inorganic compounds. World Publ. Co., Beijing

Publisher's Note

Springer Nature remains neutral with regard to jurisdictional claims in published maps and institutional affiliations.